




In Situ Measurements of Lunar Dust at the Chang'E-3 Landing Site in the Northern Mare Imbrium

Detian Li¹, Yi Wang², He Zhang³ , Jianhong Zhuang², Xiaojun Wang¹, Yongjun Wang¹ , Shengsheng Yang¹, Zezhou Sun³, Xianrong Wang², Liping Chen³, Rijian Yao², Xin Zou³, Jinan Ma³, Yang Cui², Xilai Wang², Cunhui Li² , Haiyan Zhang², Xiongyao Li⁴, Xin Gao², Xinyu Cui⁵, Biao Zhang¹, Wenfeng Li¹, and Hongyu Lin⁶

¹Science and Technology on Vacuum Technology and Physics Laboratory, Lanzhou Institute of Physics, China Academy of Space Technology, Lanzhou, China, ²Science and Technology on Material Performance Evaluating in Space Environment Laboratory, Lanzhou Institute of Physics, China Academy of Space Technology, Lanzhou, China, ³Beijing Institute of Spacecraft System Engineering, China Academy of Space Technology, Beijing, China, ⁴State Key Laboratory of Environmental Geochemistry, Institute of Geochemistry, Chinese Academy of Sciences, Guiyang, China, ⁵Tianjin Institute of Power Source, China Electric Technology Group Corporation, Tianjin, China, ⁶Beijing Institute of Space Mechanics and Electricity, China Academy of Space Technology, Beijing, China

Key Points:

- Sticky quartz crystal microbalance was used to detect lunar dust for the first time
- Annual lunar dust deposition mass in the northern Mare Imbrium was first determined
- The most probable causes for the high dust deposition rates in the first three daytimes were the activities of Yutu rover and two major meteors

Supporting Information:

- Supporting Information S1

Correspondence to:

D. Li, J. Zhuang and Y. Wang, lidetian@hotmail.com; zhuangjianhong@spacechina.com; wyjlxlz@163.com

Citation:

Li, D., Wang, Y., Zhang, H., Zhuang, J., Wang, X., Wang, Y., et al. (2019). In situ measurements of lunar dust at the Chang'E-3 landing site in the northern Mare Imbrium. *Journal of Geophysical Research: Planets*, 124, 2168–2177. <https://doi.org/10.1029/2019JE006054>

Received 23 MAY 2019

Accepted 26 JUL 2019

Accepted article online 2 AUG 2019

Published online 14 AUG 2019

Detian Li and Yi Wang contributed equally to this work.

This article was corrected on 23 AUG 2019. See the end of the full text for details.

Abstract Lunar dust is regarded as the most crucial environmental problem on the Moon, and related research has crucially important scientific and technological interests. Here, we first reported the in situ measurements of lunar dust at the Chang'E-3 landing site in the northern Mare Imbrium using temperature-controlled sticky quartz crystal microbalance. The results showed that a total deposition mass at a height of 190 cm above the lunar surface during 12 lunar daytimes in the northern Mare Imbrium was about 0.0065 mg/cm², corresponding to an annual deposition rate of ~21.4 μg/cm², which is comparable with that of Apollo's result to some extent. The present researches are strategically important for future human and robotic lunar expeditions, and can provide a valuable reference for the design of dust protection for onboard payloads long-term exposure to the lunar environment.

Plain Language Summary Apollo astronauts pointed out that “dust is the number one environmental problem on the Moon” and “dust is the number one concern in returning to the Moon.” Dust on the lunar surface can be easily levitated and transported by several natural and anthropogenic causes, which can raise several detrimental problems for exploration activities. To date, however, the reports about in situ measurements of dust on the lunar near surface are comparatively few. The sticky quartz crystal microbalance onboard Chang'E-3 was used to investigate the lunar dust deposition rate caused by natural factors, and an annual deposition rate, ~21.4 μg/cm², in the northern Mare Imbrium was determined for the first time. This work was unique as it was made on the lunar surface rather than in orbit, and this research can provide a valuable reference for the protection of the payloads from exposure to lunar dust particles for the future lunar exploration missions.

1. Introduction

It is well known that the Moon's atmosphere is extremely tenuous even though its surface is surrounded by a permanent, asymmetric dust cloud originating from the high speed micrometeoroid bombardments (Colwell et al., 2007; Horányi et al., 2015; Stern, 1999; Szalay & Horányi, 2015a; Wooden et al., 2016). On the lunar surface, dust movement can be induced by natural and anthropogenic causes such as sunrise/sunset (Grün et al., 2011; O'Brien & Hollick, 2015), astronaut/robotic activities (O'Brien, 2011), rocket launch/landing (O'Brien, 2009), solar wind (Afshar-Mohajer et al., 2015), micrometeoroid collision (Horányi et al., 2015; Szalay & Horányi, 2016; Wooden et al., 2016), and some other mechanisms not yet identified (Katzan & Edwards, 1991), which could lead to a series of detrimental problems for exploration activities, astronaut health and even mission success. For instance, the lunar passive seismometer onboard Apollo 11 was prematurely terminated by ground command as it was contaminated with dust and debris caused by the lunar module ascent rocket exhausts and overheated and failed subsequently (O'Brien, 2009). The other dangerous case was that the Apollo 15 landing was accomplished with zero surface visibility owing to the generation of large amounts of dust during landing process, as a result, the lander distinctly tilted backward 11° into a shallow crater after

landing (Metzger et al., 2008). Thus, in order to mitigate the lunar dust-related problems, provide substantial guidance for the planning of future lunar exploration even extraterrestrial settlement constructions, and offer valuable information for understanding lunar atmospheric evolution, in situ measurement of dust deposition on the lunar surface is the first step for achieving these purposes. To date, however, the reports about in situ measurements of dust on the lunar near surface are comparatively few (Berg et al., 1976; Grün & Horányi, 2013; O'Brien, 2011) even though some studies were executed from lunar orbits (Feldman et al., 2014; Glenar et al., 2014; Grava et al., 2017; Horányi et al., 2015; Szalay & Horányi, 2015b; Wooden et al., 2016). On 14 December 2013 at 21:11 (UTC + 8), Chang'E-3 (CE-3) spacecraft, the first visitor from China soft-landing on the Moon surface, successfully touched down at 44.12°N, 19.51°W on the Moon (Fa et al., 2015)—a region that was neglected by previous expeditions, which carried, among other instruments, one lunar dust detector (LDD), providing an unique opportunity to learn about the lunar dust deposition in the northern Mare Imbrium.

Here, we report in situ measurement results obtained by one sensor of LDD—sticky quartz crystal microbalance (SQCM), which was installed in a temperature-controlled cabinet mounted on the front-left corner of the CE-3 lander and devoted to detect the lunar dust principally induced by natural factors in each lunar daytime during 1-year-mission duration. The temperature-controlled cabinet was opened in sunrise period about a solar elevation of 20° and closed in sunset period about a solar elevation of 20° in each lunar daytime in order to make sure all the scientific instruments can survive and operate over the harsh low-temperature lunar night. The solar elevation corresponding to the cabinet open and close moments varied slightly from one day to another within 2° difference from the second to the twelfth lunar daytimes. The first lunar daytime was an exception, in which the cabinet door was opened at a solar elevation angle about 35°. In addition, the top cover of the temperature-controlled cabinet was closed in each lunar noon for a short time in order to avoid the excessive heating. This sensor, having a sensing area of 0.33 cm², was horizontally mounted at a height of 190 cm above the local lunar surface, and the field-of-view of SQCM sensor is a cone with a half angle of approximately 75°. The detailed installation position and working time of SQCM are given in Figure S1 and Table S1 in the supporting information, respectively. In this work, we first reported the in situ measurements of lunar dust at the CE-3 landing site in the northern Mare Imbrium using SQCM. The working principle and laboratory calibrations of SQCM are described in section 2 and then the measurement results and discussion are demonstrated in section 3, and followed by a conclusion in section 4.

2. Working Principle and Laboratory Calibrations of SQCM

QCM is a piezoelectric quartz crystal sensor that can monitor very small mass changes on the sensor surface in real-time according to its resonance frequency shift. Nowadays, the most extensively used QCM comprises an AT-cut piezoelectric quartz crystal sandwiched between two metal excitation electrodes, in which the electrodes are used to apply an alternating electric field across the thin crystal to cause the vibration of the crystal at its resonant frequency via the converse piezoelectric effect. It has been widely demonstrated that the resonant frequency shifts of QCMs are very sensitive to mass changes at the electrode surfaces, and the basic theory reflecting the relationship between the frequency change (Δf) and the mass change (Δm) was derived by Sauerbrey (1959):

$$\Delta f = -\frac{2f_0^2 \Delta m}{A\sqrt{\mu_q \rho_q}} \quad (1)$$

where Δf is the measured frequency shift, f_0 is the initial resonant frequency of the quartz crystal, Δm is the mass change, A is the piezoelectrically active area, ρ_q is the density of quartz, and μ_q is the shear modulus.

If we define $\frac{2f_0^2}{\sqrt{\mu_q \rho_q}} = S_m$, then

$$\frac{\Delta m}{A} = -\frac{\Delta f}{S_m} \quad (2)$$

Here, S_m is the mass sensitivity of the QCM sensor.

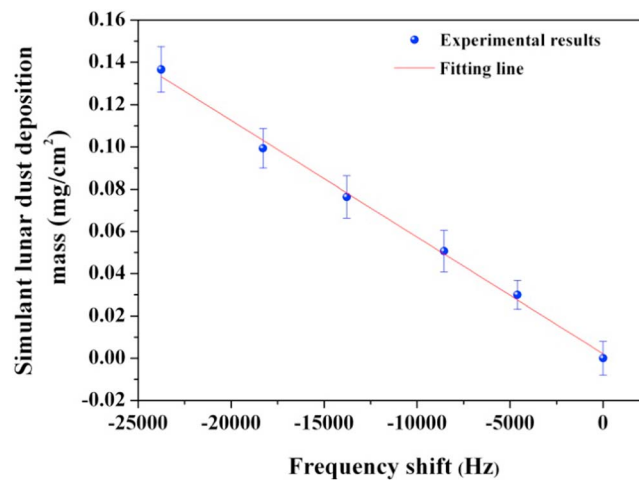


Figure 1. The lunar dust simulants deposition mass on SQCM crystal surface as a function of its frequency shift.

The QCMs have unique advantages, including low consumption, lightweight, small size, high sensitivity, for space applications, and the utilizations of QCMs in space missions have been well demonstrated in previous works (Colangeli et al., 2007; Wood et al., 2001). However, QCM cannot be directly used to detect lunar dust simulants due to the fact that the binding force between the electrode and the dust simulants is not strong enough to make them oscillate together with identical frequency. In reality, the strong cohesive forces within the lunar dust itself are large enough possible to hold them together, just as demonstrated by Gold (Gold, 1971), which can assure that the lunar dust particles next to the lowest deposition layer is able to oscillate with the beneath deposition layer together. On the other hand, the lunar dust could stick to any surface with which it came in contact. However, it can be inferred from Apollo 12 experiences that the cohesive forces between the lunar dust particles and payload surface (solar cell surface) was not very strong because the lunar dust deposited on the vertical east facing solar cell during the first lunar day was partially removed (50%) at the time of lunar module ascent by rocket exhausts, and totally removed by natural causes before the midmorning of the second lunar day (O'Brien, 2009), indicating that the cohesive forces between the lunar dust particles and payload surfaces were not very strong. Thus, in our case, the QCM electrode was covered by a thin layer sticky film (to be a sticky QCM, named SQCM) to enhance the binding strength between the electrode and the dust particles. The parent QCM used in this work comprised a 10-MHz AT-cut quartz-plate crystal with two gold electrodes, and the sticky film was coated on the top electrode to capture the lunar dust simulants. Here, the used sticky film was Apiezon H vacuum grease, which is a silicone-free low vapor pressure vacuum grease and possesses good stiction over a wide temperature range from -65 to 140 °C. The coated sticky film leads to the decrease of reference frequency of SQCM, and a value of ~ 9.97329562 MHz was obtained, which is slightly less than the initial 10 MHz. However, the ratio of frequency change (Δf) and initial resonant frequency (f_0) of the resultant SQCM equals to 0.0027, which is less than 0.05, indicating the SQCM can still work well (Huang et al., 2010).

The original relation between mass change and resonant frequency shift of the resultant SQCM was changed owing to the addition of sticky film, and thus, a new calibration was carried out in order to determine the new function relation between them by using lunar dust simulant. Here, it should be pointed out that the used simulant was developed by the Institute of Geochemistry Chinese Science Academy, which contains ~ 75 vol.% of glass, ~ 15 vol.% of plagioclase and 10 vol.% of olivine, pyroxene, ilmenite, and nanophase Fe^0 . The nanophase Fe^0 imparts magnetic properties of the lunar dust but might not be strong enough to affect the operation of the SQCM instrument, as the SQCM is a piezoelectric quartz crystal sensor, in which the mechanical energy and electrical energy are transformed into each other. The median particle size of the used lunar dust simulants is about 500 nm, whose size is closer to the real lunar dust relative to JSC-1Avf (Park, et al., 2008; Liu & Taylor, 2011). These characteristics of the used lunar dust simulants are well matched with that of lunar dusts, and more detailed information about the used lunar dust simulants was described in Tang et al. (2017). The calibration experiments were performed using a dust spray

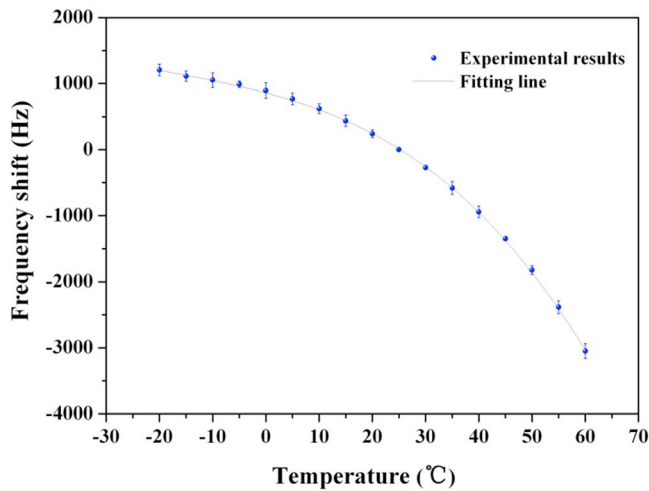


Figure 2. The frequency shift of sticky quartz crystal microbalance as a function of sensor temperature. The black line is obtained from the third-order polynomial fitting of the experimental data.

simulation equipment apparatus. The calibration temperature and pressure of the simulation equipment are 25 °C and $\sim 10^{-3}$ Pa, respectively, and the temperature was measured by platinum resistance temperature sensor, as shown in Figure S1. The dust simulant was released by a steel brush during the experiment processes, and the released dust mass was controlled by motor speed and working time. The deposition mass on the SQCM was determined as follows: Four aluminum foils with $1 \times 1\text{-cm}^2$ area were placed around the SQCM, and the mass on the SQCM was determined by averaging over the deposition mass on the four aluminum foils. The deposition mass on the foils was weighted by the foil before and after dust deposition by a high-precision electronic balance (METTLER-TOLEDO XP2U) with $0.1\text{-}\mu\text{g}$ readability. The mass change as a function of frequency shift is exhibited in Figure 1.

It is seen from above figure that dust deposition mass linearly increases with frequency shift from 0 to ~ 25000 Hz, and the ratio $\Delta f/f_0$ is still less than 0.05 even the Δf is as large as 25000 Hz, implying the SQCM can work well. The black line is obtained from the linear fitting of the experimental data, and the fitted formula is given as follows:

$$\Delta m = -5.63 \times 10^{-6} \cdot \Delta f \quad (4)$$

Here, Δm is mass change on SQCM in unit area in milligrams per square centimeter, Δf is frequency shift of the SQCM in Hertz. The mass sensitivity of the resultant SQCM sensor is $5.63 \times 10^{-6} \text{ mg}/(\text{cm}^2 \cdot \text{Hz})$.

It is well known that the QCM sensors are very sensitive to insert light after solar and are usually placed in a thermally stabilized measurement chamber. In practical in situ measurement on the lunar surface, the SQCM was strategically installed in a temperature-controlled cabinet to block the solar light, however, the actual temperature in the cabinet varied from -10 to 50 °C during in situ measurement process. Thus, the resonant frequency shifts of the SQCM sensor as a function of temperature was determined in the laboratory in advance. The actual temperature variation of SQCM sensor during in situ measurement process on the lunar surface was given in Figure S2.

Figure 2 demonstrates the frequency shift of SQCM as a function of sensor temperature. Here, the reference frequency of SQCM at a temperature of 25 °C was ~ 9973295.62 Hz, and the frequency shifts under other temperatures were obtained by the corresponding frequency under studied temperatures minus the reference frequency. The frequency measurements at each studied temperature were conducted several times, and the averaged values as well as standard deviations of frequency are given in Figure 2. The black line was obtained by fitting the experiment data, and the fitted formula for present data is as follows:

$$\Delta f = 873.24 - 21.27t - 0.36t^2 - 0.006t^3 \quad (5)$$

This formula will be used to modify the resonant frequency shift obtained at different temperatures during actual in situ measurements on the lunar surface, and the resonant frequency shift corrected by using equation (5) is defined as normalized frequency, in which the frequency shift caused by temperature was eliminated.

In order to make sure that the coated sticky film can still work in the lunar environment after 1-year-mission period, a series of evaluation experiments, including high- and low-temperature measurement, ultraviolet irradiation, ionizing irradiation, and mass loss measurement, were performed subsequently on the ground. (1) The high- and low-temperature cycle tests were conducted in air in order to estimate the stiction of the used sticky film in low-temperature stage, and the cycle experiment was defined as follows: 25 °C \rightarrow -65 °C \rightarrow 25 °C, in low-temperature stage, the temperature was kept constant for 48 hr. The high- and low-temperature cycle tests were conducted 30 times in total. (2) The ultraviolet irradiation experiments were carried out in air at room temperature in a simulation system, and the typical ultraviolet energy flux at the sticky film position was determined to be about quintuple of the solar constant, and the irradiation intensity and

time were ~ 48 kcal/cm² and 42 days, respectively, being equivalent to 210 Sun days. (3) The ionizing irradiation experiments were executed using ⁶⁰Co γ ray with 1.25-MeV energy, the irradiation dose was 10^5 rad (Si)/hr, and irradiation time is 10 hr, and the total irradiation dose was equal to that of 1 year received on the lunar surface. (4) The mass loss measurement experiments were carried out in a vacuum environment ($\sim 10^{-4}$ Pa) with a temperature of 125 °C, and the total mass loss rate is 4.9% after 252 hr test. After these evaluation experiments, the SQCM coated with fresh sticky film and the one coated with treated sticky film exhibited similar frequency response to the deposited lunar dust simulants, indicating that the sticky film can still work after 1-year-mission duration on the lunar surface environment.

3. In Situ Measurement Results and Discussion

The lunar surface is mainly covered with a thick layer of fine dust particles generated by continuous meteoroid bombardment over the past billion years, in which the finest dust particles with size less than 20 μ m can be easily levitated and transported on the lunar surface by several mentioned-above mechanisms (Katzan & Edwards, 1991; O'Brien, 2011; O'Brien & Hollick, 2015). It was revealed by scientific payloads onboard CE-3 mission that the CE-3 landing site is a relatively young high-titanium mare basalt region characterized by thin regolith and numerous small craters, which is compositionally different from the several Apollo landing sites (Xiao et al., 2015; Zhang et al., 2015). Although the dust transport mechanisms are closely correlated to the regolith composition (Glenar et al., 2014), similar to Apollo landing cases, the CE-3 7500 N lander engine exhausted large amounts of propellant during descent stage, which also, as a result, kicked up a lot of dust (as demonstrated in Figure S3), posing a promising challenge to photo-sensitive and thermo-sensitive devices.

To accurately determine the dust deposition mass on lunar surface, SQCM was calibrated and characterized in ground experiments as demonstrated above, and the corresponding relationships between mass change and sensor temperature and resonant frequency shift of SQCM were determined in advance (Figures 1 and 2), respectively. Thus, at present, once the frequency shift and the corresponding temperature were determined from measurements on the lunar surface, the lunar dust deposition mass can be directly derived using the above built relationships. In view of the fact that SQCM mainly interested in the dust induced by natural causes, the dust shield of SQCM was opened until 16 December 2013 at 03:46 (UTC + 8), ~ 30 hr after CE-3 landing, in order to reduce the influence of CE-3 landing as much as possible. The detailed variation of lunar dust deposition mass in the first four lunar daytimes is depicted in Figure 3.

Figure 3 demonstrates the detailed variation of the lunar dust deposition mass during the first four lunar daytimes. The averaged deposition mass from the first lunar daytime to the fourth one increases subsequently, indicating that the total deposition mass increases as a function of testing time. However, the lunar dust deposition mass in each lunar daytime shows an obvious fluctuation rather than monotonous increase versus time, which is mainly due to the fact that the platinum resistance temperature sensor did not directly contact with the quartz crystal plate (if so, the temperature sensor would affect the operation of the SQCM sensor), which is several millimeter away from the quartz crystal plate. Thus, the temperature obtained by the sensor was somewhat different from SQCM plate temperature, in other words, the measured temperature by temperature sensor lagged behind SQCM plate temperature. However, our critical result, the annual deposition mass of lunar dust, still holds because it was averaged over the temperatures in each lunar daytime. In order to further investigate this issue, the detailed variation of temperature, raw frequency, and normalized frequency of SQCM sensor during the first four lunar daytimes is given in Figure 4.

Figure 4 shows the detailed variation of temperature, raw frequency and normalized frequency of SQCM sensor during the first four lunar daytimes. It is clearly shown that the resonant frequency of SQCM is strongly dependent upon temperature. Taking the first lunar daytime as an example (Figure 4a), in the low-temperature section, ~ 25 °C, the resonant frequency is about 9973260 Hz, while in the high-temperature section, ~ 37 °C, the resonant frequency is about 9972600 Hz, and hence, the discrepancy of resonant frequency between the low- and high-temperature sections in the first lunar daytime is as high as 660 Hz. However, the significant discrepancy was partially corrected by taking into account the contribution of temperature. As also demonstrated in Figure 4a, for example, the normalized frequency in the low-temperature section (~ 25 °C) in the first lunar daytime is about 9973270 Hz, and this value is 9973310 Hz in the corresponding high-temperature section (~ 37 °C), and the discrepancy of normalized frequency is reduced to 40 Hz in this case. Of course, similar trends were also observed in other lunar daytimes. In reality, the

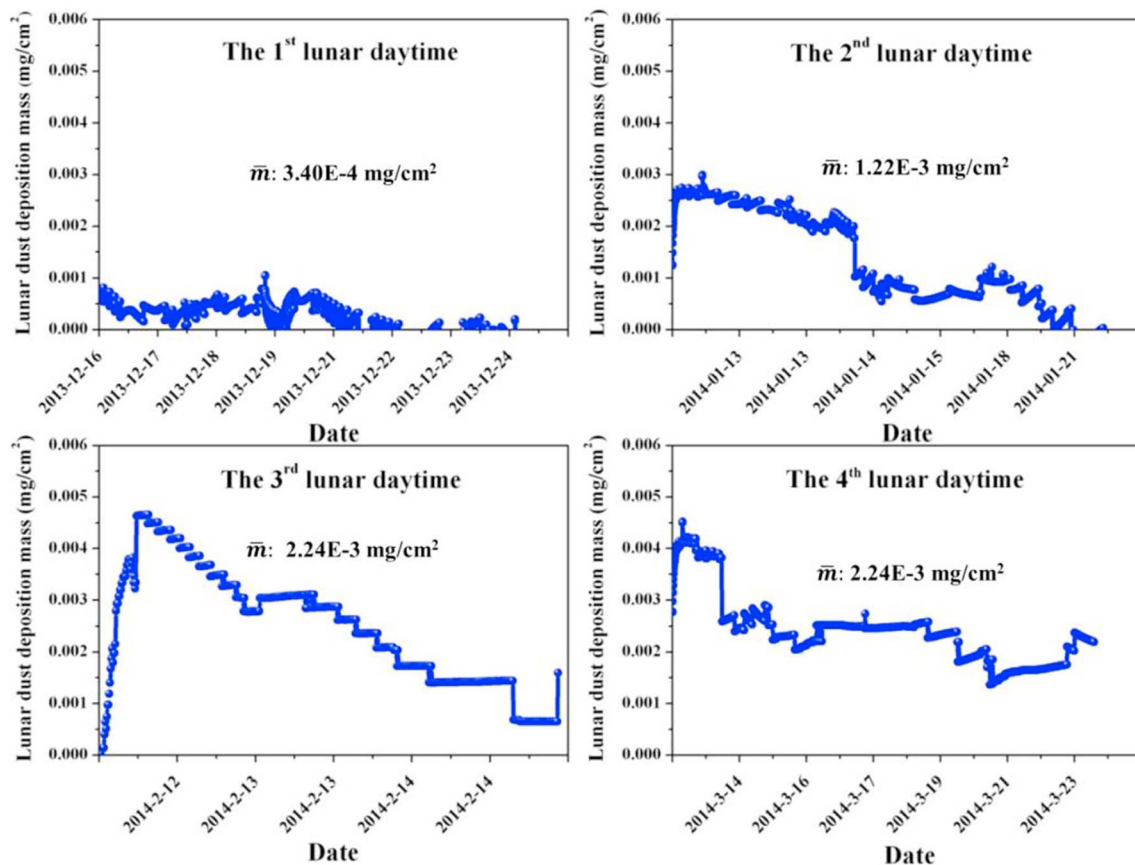


Figure 3. The detailed variation of lunar dust deposition mass during the course of each of the first four lunar daytimes, where \bar{m} represents the averaged lunar dust deposition mass in the corresponding lunar daytime. The data acquisition of sticky quartz crystal microbalance follows the main payload's working time, and the working time of main payloads become less and less from the first to the last lunar daytimes, and thus, the data points in the later several lunar daytimes are relatively less.

lunar dust deposition mass in each lunar daytime during the whole detection period was averaged over all the measurement points owing to the significant fluctuation of resonant frequency, and the final results are shown in Figure 5.

It can be seen from Figure 5a that as time increases the lunar dust deposition mass on SQCM gradually increases with obvious fluctuation, and a total deposition mass about 0.0065 mg/cm^2 was achieved for ~ 12 lunar daytimes. Here, it should be noted that the actual deposition time of lunar dust on SQCM in 1-year duration is only slightly less than one third year (Table S1), and thus, an annual deposition rate of lunar dust in the northern Mare Imbrium is $\sim 21.4 \mu\text{g/cm}^2$. Up to now, only a few results about lunar dust deposition rate on the lunar surface can be available from previous works to compare with our value (Hollick & O'Brien, 2013; Rennilson & Criswell, 1974). According to the prevailing viewpoint, the two dominant natural factors accounting for dust transport and deposition on the lunar surface, what are SQCM interested in, are micrometeoroid impacts and electrostatic transport (Afshar-Mohajer et al., 2015). The lunar dust deposition rate induced by micrometeoroid impacts, including primary and secondary impacts, on lunar surface was estimated to be $\sim 10 \mu\text{g/cm}^2/\text{year}$ (Katzan & Edwards, 1991). However, as for the lunar dust deposition rate caused by the second main natural factor—electrostatic transport, a high deposition rate, as high as $3 \times 10^4 \mu\text{g/cm}^2/\text{year}$, was presumed by Rennilson and Criswell (1974). This value was not relevant according to the subsequent studies, and the actual lunar dust deposition rate caused by electrostatic transport should be considerably lower than the value obtained by Rennilson and Criswell, as pointed out by Gaier (Gaier & Jaworske, 2007). Recently, Hollick and O'Brien revisited and reanalyzed the Apollo Dust Detector Experiments (DDEs) data accumulated over 7 years on the lunar surface, and according to their research the upper limit of deposition rate of lunar dust induced by both

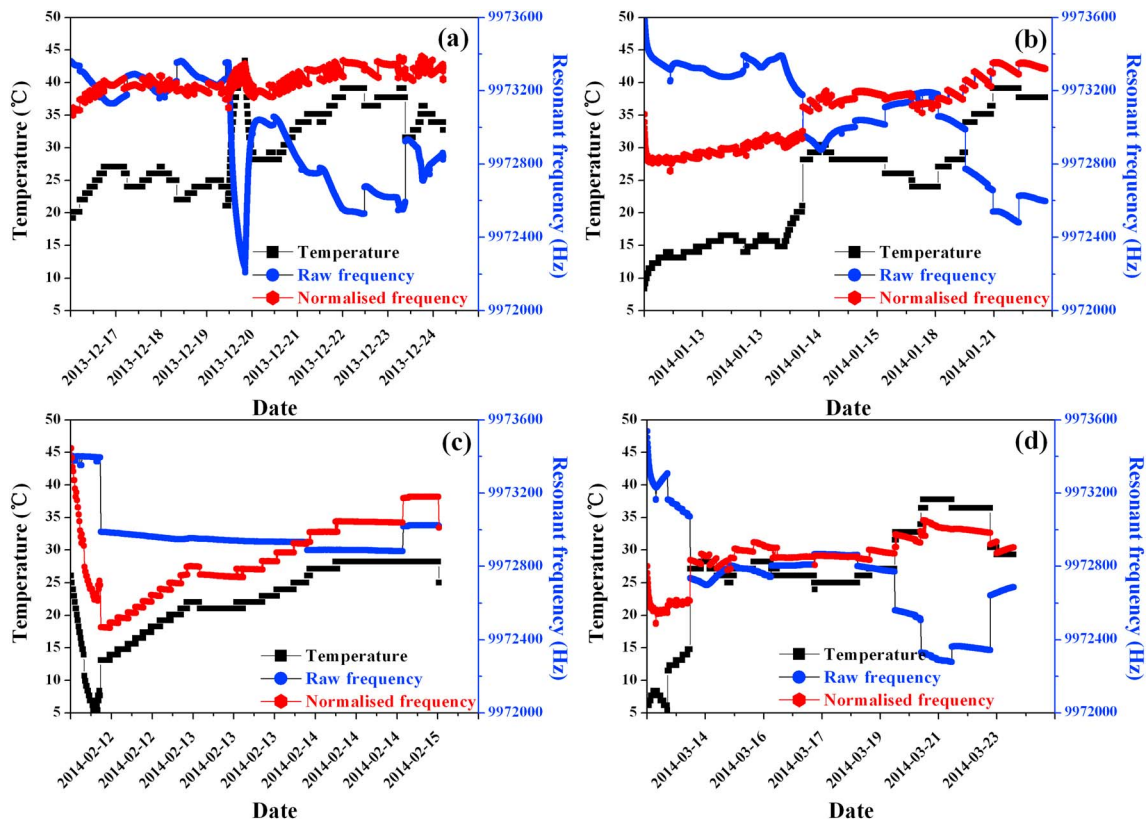


Figure 4. The detailed variation of temperature (black), raw frequency (blue), and normalized frequency (red) of sticky quartz crystal microbalance sensor from the first lunar daytime (a) to the fourth lunar daytime (d), subsequently.

natural and anthropogenic causes on the lunar surface was reckoned to be $100 \mu\text{g}/\text{cm}^2/\text{year}$ (Hollick & O'Brien, 2013). Our result, falling in the Apollo's range, is somewhat less than Apollo's upper limit, which is mainly attributed to the fact that, on one hand, the lunar dust was directly generated as a result of long-term space weathering on the lunar surface, taking place continuously once it formed (Tang et al., 2017). The CE-3 landing site is on the continuous ejecta deposits of a fresh impact crater (named Zi Wei) formed ~ 27 to ~ 100 million years ago (Fa et al., 2015; Ling et al., 2015; Xiao et al., 2015), which is younger than the Apollo 12 landing site (the Apollo 12 landing site was on the northwest rim of a 200-m-diameter impact crater formed 240 million years ago; Funkhouser, 1971), and thus, the CE-3 landing site was much less weathered in contrast to Apollo 12 landing site. As a result, fewer lunar dust particles were formed in CE-3 landing site due to the less space weathering time relative to Apollo 12, and thus, a low annual deposition rate was obtained in CE-3 landing site. On the other hand, spacecraft launch is the most significant factor for local lunar dust transport from the source. In Apollo cases, the lunar modules were launched from the Moon surface once their missions were completed. Thus, large amounts of dust would be stirred up by the rocket exhaust during launch process. As a result, more lunar dust would be deposited on the DDE surfaces in contrast to CE-3 because the latter has no launch process from the lunar surface. Third, in Apollo's experiments the deposition rate of lunar dust was derived from the short-circuit current degradation of solar cell; however, the short-circuit current of solar cell was correlated with size, shape and distribution of the accumulated lunar dust on cell surfaces (Katzan & Edwards, 1991), the authors assumed that the accumulated lunar dust particles in the 20- to $38\text{-}\mu\text{m}$ size range uniformly distributed on the solar cell surface (Hollick & O'Brien, 2013), which was at most an approximate case for actual situation on the lunar surface. Fortunately, such dependence was consciously avoided in SQCM, in which the frequency shift has nothing to do with the size and shape of deposited lunar dust. Therefore, in this sense, the result obtained by SQCM was probably more accurate than that of Apollo's results. In addition, the different installation heights of SQCM (~ 190 cm) and DDE (~ 100 cm) could be also responsible for the discrepancy of lunar dust deposition mass.

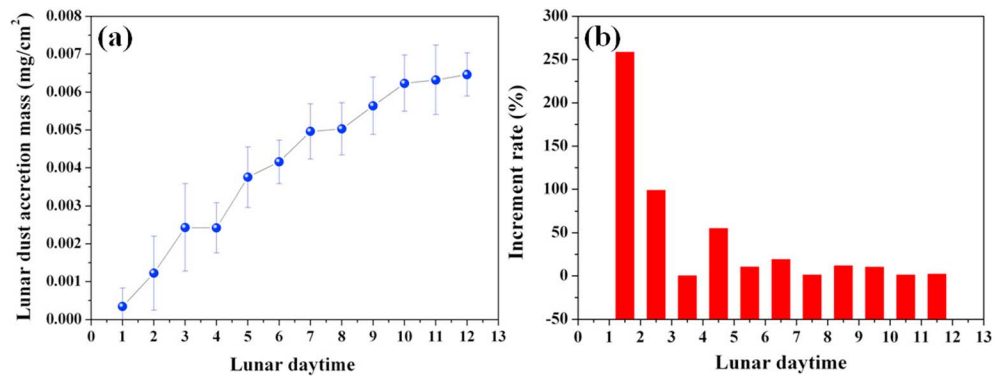


Figure 5. (a) The variation trends of averaged lunar dust deposition mass during the 1-year-mission detection period. The error bars represent the standard deviation of lunar dust deposition mass. (b) The lunar dust increment rate in each lunar daytime is exhibited. Here, the increment rate was defined as follows: The lunar dust deposition mass in the first daytime and second lunar daytime are A and B , respectively, then the increment rate between the consecutive two lunar daytimes is $(B - A)/A \times 100\%$. The bar between Lunar daytimes 1 and 2 represents the increment rate between the two lunar daytimes.

The lunar dust deposition mass on the SQCM in each lunar daytime varied obviously over the 1-year-mission duration, as demonstrated in Figure 5b. The deposition mass in the first lunar daytime, as expected, was relatively little, which was mainly ascribed to the shorter deposition time in this lunar daytime in contrast to other ones. In the first lunar day, the CE-3 landed in the morning and the SQCM was opened to measure the lunar dust with a solar elevation angle about 35° . However, in other lunar daytimes, SQCM started to work with a solar elevation angle about 20° . Consequently, the deposition time in the first lunar daytime was 46 hr less than that of other lunar daytimes, and thus, little deposition mass was obtained in the first lunar daytime. The increment rate of lunar dust deposition mass in consecutive two lunar daytimes is exhibited in Figure 5b. It can be seen that the increment rate in the first three lunar daytimes is relatively high, and then it remained relatively low and constant value, particularly for the last seven lunar daytimes. The accurate causes for the high increment rate over the first lunar daytimes are not yet understood in our case. It has been pointed out that the robotic activity on the lunar surface and the occurrences of meteor shower during the detection period can induce the movement of lunar dust (Colaprete et al., 2016; Katzan & Edwards, 1991); thus, the most probable causes for the high dust deposition rates in the first three daytimes were the activities of Yutu rover (Xiao et al., 2015) and two major meteor (Colaprete et al., 2016) occurred during that time period. However, combined with the detailed variation of lunar dust deposition mass in the first four lunar daytimes (Figure 4), it is hard to accurately determine whether or not the Yutu rover as well as the meteor shower could contribute to the high increment rate because the obvious fluctuation of resonant frequency could have overwhelmed a potential contributions from them. In addition, O'Brien et al. presented a minimalist qualitative model of lunar surface dust transport (O'Brien & Hollick, 2015). In that model, they believed that the lunar dust particles disrupted by rocket exhaust gases via penetrating into the dust layer, which was freed from strong particle-to-particle cohesive force, could be levitated to a certain height due to the electrostatic repulsion of like-charged objects during the next few sunrises. In our case, however, SQCM was in a temperature-controlled cabinet, the sensor did not work when the sunrise/sunset terminators passed by the CE-3 landing site. Thus, it is impossible to verify this recently developed qualitative model. This phenomenon should be further investigated to understand what is/are responsible for the high increment rate of lunar dust over the first few lunar daytimes.

4. Conclusions

In this work, the lunar dust at CE-3 landing site in the northern Mare Imbrium was detected in situ for the first time by a temperature-controlled SQCM onboard the CE-3 lunar probe between December 2013 to December 2014. The correlations between the sensor temperature, lunar dust simulant deposition mass and the resonant frequency shifts of SQCM were determined in the laboratory in advance. The used SQCM with 5.63×10^{-6} mg/(cm²·Hz) mass sensitivity worked from a solar elevation of around 20° near sunrise to 20° near sunset in each lunar daytime except two days in which the total lunar eclipses occurred. It

was found from our measurements that a total deposition mass caused by natural causes in the northern Mare Imbrium at a height of 190 cm during 12 lunar daytimes was about 0.0065 mg/cm², corresponding to an annual deposition rate of ~21.4 μg/cm², which was less than the upper limit obtained from Apollo's explorations. The main sources of this discrepancy were as follows: On one hand, the lunar dust particles in CE-3 landing site were relatively less abundantly in amounts in contrast to the Apollo's sites as the CE-3 landing site was much less weathered than the Apollo's sites. On the other hand, the different working principles for LDDs onboard both CE-3 and Apollo missions were also responsible for the formation of this discrepancy to some degree. This work was unique as it was made on the lunar surface rather than in orbit, and this research can provide a valuable reference for the protection of the payloads from exposure to lunar dust particles for the future lunar exploration missions.

Acknowledgments

The authors wish to thank Brian J. O'Brien and an anonymous reviewer for their insightful suggestions in evaluating this manuscript, which led to many improvements in the manuscript. All the authors acknowledge State Key Laboratory of Environmental Geochemistry for providing their lunar dust simulants. All the data used in this paper can be obtained from https://www.researchgate.net/publication/334466274_JGR-Planets_Original_data_website. Funding: Detian Li and Yongjun Wang acknowledge support of the Natural Science Foundation of China (Grants 61627805 and 61671226). Yongjun Wang thanks to the Equipment Pre-Research Foundation of Equipment Development Department of People's Republic of China Central Military Commission (Grant 6142207010704). The cover image comes from Lunar Exploration and Space Engineering Center of China National Space Administration.

References

- Afshar-Mohajer, N., Wu, C. Y., Curtis, J. S., & Gaier, J. R. (2015). Review of dust transport and mitigation technologies in lunar and Martian atmospheres. *Advances in Space Research*, 56(6), 1222–1241. <https://doi.org/10.1016/j.asr.2015.06.007>
- Berg, O. E., Wolf, H., & Rhee, J. (1976). Lunar soil movement registered by the Apollo 17 cosmic dust experiment. In H. Elsaesser, & H. Fechtig (Eds.), *Interplanetary Dust and Zodiacal Light, Lect. Notes Phys.* (Vol. 48, pp. 233–237). Berlin: Springer.
- Colangeli, L., Lopez-Moreno, J. J., Palumbo, P., Rodriguez, J., Cosi, M., Corte, V. D., et al. (2007). The Grain Impact Analyser and Dust Accumulator (GIADA) experiment for the Rosetta mission: Design, performances and first results. *Space Science Reviews*, 128(1–4), 803–821. <https://doi.org/10.1007/s11214-006-9038-5>
- Colaprete, A., Sarantos, M., Wooden, D. H., Stubbs, T. J., Cook, A. M., & Shirley, M. (2016). How surface composition and meteoroid impacts mediate sodium and potassium in the lunar exosphere. *Science*, 351(6270), 249–252. <https://doi.org/10.1126/science.aad2380>
- Colwell, J. E., Batiste, S., Horányi, M., Robertson, S., & Sture, S. (2007). Lunar surface: Dust dynamics and regolith mechanics. *Reviews of Geophysics*, 45, RG2006. <https://doi.org/10.1029/2005RG000184>
- Fa, W., Zhu, M.-H., Liu, T., & Plescia, J. B. (2015). Regolith stratigraphy at the Chang'E-3 landing site as seen by lunar penetrating radar. *Geophysical Research Letters*, 42, 179–187. <https://doi.org/10.1002/2015GL066537>
- Feldman, P. D., Glenar, D. A., Stubbs, T. J., Retherford, K. D., Randall Gladstone, G., Miles, P. F., et al. (2014). Upper limits for a lunar dust exosphere from far-ultraviolet spectroscopy by LRO/LAMP. *Icarus*, 233, 106–113.
- Funkhouser, J. (1971). Noble gas analysis of KREEP fragments in lunar soil 12033 and 12070. *Earth and Planetary Science Letters*, 12, 263–272.
- Gaier, J. R., and D. A. Jaworske (2007), Lunar dust on heat rejection system surfaces: Problems and prospects, AIP Conference Proceedings, 880, 27–34.
- Glenar, D. A., Stubbs, T. J., Hahn, J. M., & Wang, Y. (2014). Search for a high-altitude lunar dust exosphere using Clementine navigational star tracker measurements. *Journal of Geophysical Research: Planets*, 119, 2548–2567. <https://doi.org/10.1002/2014JE004702>
- Gold, T., (1971), Lunar-surface close-up stereoscopic photography, Apollo 14 Preliminary Science Report, NASA SP-272, Washington, DC.
- Grava, C., Stubbs, T. J., Glenar, D. A., Retherford, K. D., & Kaufmann, D. E. (2017). Absence of a detectable lunar nanodust exosphere during a search with LRO's LAMP UV imaging spectrograph. *Geophysical Research Letters*, 44, 4591–4598. <https://doi.org/10.1002/2017GL072797>
- Grün, E., & Horányi, M. (2013). A new look at Apollo 17 LEAM data: Nighttime dust activity in 1976. *Planetary and Space Science*, 89, 2–14.
- Grün, E., Horányi, M., & Sternovsky, Z. (2011). The lunar dust environment. *Planetary and Space Science*, 59, 1672–1680.
- Hollick, M., & O'Brien, B. J. (2013). Lunar weather measurements at three Apollo sites 1969–1976. *Space Weather*, 11, 651–660. <https://doi.org/10.1002/2013SW000978>
- Horányi, M., Szalay, J. R., Kempf, S., Schmidt, J., Grün, E., Srama, R., & Sternovsky, Z. (2015). A permanent, asymmetric dust cloud around the Moon. *Nature*, 522, 324–326.
- Huang, J., Jiang, Y., Du, X., & Bi, J. (2010). A new siloxane polymer for chemical vapor sensor. *Sensors and Actuators, B: Chemical*, 146(1), 388–394. <https://doi.org/10.1016/j.snb.2010.02.010>
- Katzan, C. M., and J. L. Edwards (1991), Lunar dust transport and potential interactions with power system components, NASA Contractor Rep., 4404, United States.
- Ling, Z., Jolliff, B. L., Wang, A., Li, C., Liu, J., Zhang, J., et al. (2015). Correlated compositional and mineralogical investigations at the Chang'E-3 landing site. *Nature Communications*, 6(1), 8880–8888. <https://doi.org/10.1038/ncomms9880>
- Liu, Y., & Taylor, L. A. (2011). Characterization of lunar dust and a synopsis of available lunar simulants. *Planetary and Space Science*, 59, 1769–1783.
- Metzger, P. T., Lane, J. E., Immer, C. D., & Clements, S. (2008). Cratering and blowing soil by rocket engines during lunar landings, in 6th International Conference on Case Histories in Geotechnical Engineering. In H. Benaroya (Ed.), *Lunar settlements*, (pp. 551–576). Arlington: CRC Press.
- O'Brien, B. (2009). Direct active measurements of movements of lunar dust: Rocket exhausts and natural effects contaminating and cleansing Apollo hardware on the Moon in 1969. *Geophysical Research Letters*, 36, L09201. <https://doi.org/10.1029/2008GL037116>
- O'Brien, B. J. (2011). Review of measurements of dust movements on the Moon during Apollo. *Planetary and Space Science*, 59, 1708–1726.
- O'Brien, B. J., & Hollick, M. (2015). Sunrise-driven movements of dust on the Moon: Apollo 12 Ground-truth measurements. *Planetary and Space Science*, 119, 194–199.
- Park, J., Liu, Y., Kihm, K. D., & Taylor, L. A. (2008). Characterization of lunar dust for toxicological studies. I: Particle size distribution. *Journal of Aerospace Engineering*, 21, 266–271. [https://doi.org/10.1061/\(ASCE\)0893-1321\(2008\)21:4\(266\)](https://doi.org/10.1061/(ASCE)0893-1321(2008)21:4(266))
- Rennilson, J. J., & Criswell, D. R. (1974). Surveyor observations of lunar horizon-glow. *The moon*, 10, 121–142.
- Sauerbrey, G. (1959). Verwendung von Schwingquarzen zur Wägung dünner Schichten und zur Mikrowägung. *Zeitschrift für Physik*, 155, 206–222.
- Stern, S. A. (1999). The lunar atmosphere: History, status, current problems, and context. *Reviews of Geophysics*, 37, 453–491.
- Szalay, J. R., & Horányi, M. (2015a). Annual variation and synodic modulation of the sporadic meteoroid flux to the Moon. *Geophysical Research Letters*, 42, 580–584. <https://doi.org/10.1002/2015GL066908>

- Szalay, J. R., & Horányi, M. (2015b). The search for electrostatically lofted grains above the Moon with the Lunar Dust Experiment. *Geophysical Research Letters*, *42*, 5141–5146. <https://doi.org/10.1002/2015GL064324>
- Szalay, J. R., & Horányi, M. (2016). Lunar meteoritic gardening rate derived from in situ LADEE/LDEX measurements. *Geophysical Research Letters*, *43*, 4893–4898. <https://doi.org/10.1002/2016GL069148>
- Tang, H., Li, X., Zhang, S., Wang, S., Liu, J., Li, S., et al. (2017). A lunar dust simulant: CLDS-i. *Advances in Space Research*, *59*, 1156–1160.
- Wood, B. E., Bertrand, W. T., Lesho, J. C., Uy, O. M., Green, B. D., & Hall, D. F. (2001). Midcourse Space Experiment (MSX) satellite measurements of contaminant films using QCMs—5 years in space. AIAA 2001-2956, 35th Thermophysics Conference, Anaheim, CA, 11-14.
- Wooden, D. H., Cook, A. M., Colaprete, A., Glenar, D. A., Stubbs, T. J., & Shirley, M. (2016). Evidence for a dynamic nanodust cloud enveloping the Moon. *Nature Geoscience*, *9*, 665–668.
- Xiao, L., Zhu, P., Fang, G., Xiao, Z., Zou, Y., Zhao, J., et al. (2015). A young multilayered terrane of the northern Mare Imbrium revealed by Chang'E-3 mission. *Science*, *347*(6227), 1226–1229. <https://doi.org/10.1126/science.1259866>
- Zhang, J., Yang, W., Hu, S., Lin, Y., Fang, G., Li, C., et al. (2015). Volcanic history of the Imbrium basin: A close-up view from the lunar rover Yutu. *Proceedings of the National Academy of Sciences of the United States of America*, *112*(17), 5342–5347. <https://doi.org/10.1073/pnas.1503082112>

Erratum

In the originally published version of this paper, there was an error in the text of the fifth paragraph of the In Situ Measurement Results and Discussion section. This error has since been corrected and this may be considered the authoritative version of record.